

Basler piA1900-32gm



Camera Specification

Measurement protocol using the EMVA Standard 1288

Document Number: BD000427

Version: Preliminary

Release Date: June 11, 2010

PRELIMINARY VERSION



For customers in the U.S.A.

This equipment has been tested and found to comply with the limits for a Class A digital device, pursuant to Part 15 of the FCC Rules. These limits are designed to provide reasonable protection against harmful interference when the equipment is operated in a commercial environment. This equipment generates, uses, and can radiate radio frequency energy and, if not installed and used in accordance with the instruction manual, may cause harmful interference to radio communications. Operation of this equipment in a residential area is likely to cause harmful interference in which case the user will be required to correct the interference at his own expense.

You are cautioned that any changes or modifications not expressly approved in this manual could void your authority to operate this equipment.

The shielded interface cable recommended in this manual must be used with this equipment in order to comply with the limits for a computing device pursuant to Subpart J of Part 15 of FCC Rules.

For customers in Canada

This apparatus complies with the Class A limits for radio noise emissions set out in Radio Interference Regulations.

Pour utilisateurs au Canada

Cet appareil est conforme aux normes Classe A pour bruits radioélectriques, spécifiées dans le Règlement sur le brouillage radioélectrique.

Life Support Applications

These products are not designed for use in life support appliances, devices, or systems where malfunction of these products can reasonably be expected to result in personal injury. Basler customers using or selling these products for use in such applications do so at their own risk and agree to fully indemnify Basler for any damages resulting from such improper use or sale.

Warranty Note

Do not open the housing of the camera. The warranty becomes void if the housing is opened.

All material in this publication is subject to change without notice and is copyright Basler Vision Technologies.

Contacting Basler Support Worldwide

Europe:

Basler AG
An der Strusbek 60 - 62
22926 Ahrensburg
Germany
Tel.: +49-4102-463-500
Fax.: +49-4102-463-599
bc.support.europe@baslerweb.com

Americas:

Basler, Inc.
855 Springdale Drive, Suite 160
Exton, PA 19341
U.S.A.
Tel.: +1-877-934-8472
Fax.: +1-610-280-7608
bc.support.usa@baslerweb.com

Asia:

Basler Asia Pte. Ltd
8 Boon Lay Way
03 - 03 Tradehub 21
Singapore 609964
Tel.: +65-6425-0472
Fax.: +65-6425-0473
bc.support.asia@baslerweb.com

www.baslerweb.com

Contents

1	Overview	7
2	Introduction	8
3	Basic Information	9
3.1	Illumination	10
3.1.1	Illumination Setup for the Basler Camera Test Tool	10
3.1.2	Measurement of the Irradiance	10
4	Characterizing Temporal Noise and Sensitivity	11
4.1	Basic Parameters	11
4.1.1	Total Quantum Efficiency	11
4.1.2	Temporal Dark Noise	13
4.1.3	Dark Current	14
4.1.4	Doubling Temperature	14
4.1.5	Inverse of Overall System Gain	15
4.1.6	Inverse Photon Transfer	16
4.1.7	Saturation Capacity	17
4.1.8	Spectrogram	18
4.1.9	Non-Whiteness Coefficient	21
4.2	Derived Data	22
4.2.1	Absolute Sensitivity Threshold	22
4.2.2	Signal-to-noise Ratio	23
4.2.3	Dynamic Range	25
4.3	Raw Measurement Data	26
4.3.1	Mean Gray Value	26
4.3.2	Variance of the Temporal Distribution of Gray Values	27
4.3.3	Mean of the Gray Values Dark Signal	28
4.3.4	Variance of the Gray Value Temporal Distribution in Darkness	29
4.3.5	Light Induced Variance of the Temporal Distribution of Gray Values	30
4.3.6	Light Induced Mean Gray Value	31
4.3.7	Dark Current Versus Housing Temperature	32
5	Characterizing Total and Spatial Noise	33
5.1	Basic Parameters	33
5.1.1	Spatial Offset Noise	33
5.1.2	Spatial Gain Noise	34
5.1.3	Spectrogram Spatial Noise	35
5.1.4	Spatial Non-whiteness Coefficient	38
5.2	Raw Measurement Data	39
5.2.1	Standard Deviation of the Spatial Dark Noise	39
5.2.2	Light Induced Standard Deviation of the Spatial Noise	40

Bibliography

41

1 Overview

Basler piA1900-32gm				
Item	Symbol	Typ. ¹	Unit	Remarks
Temporal Noise Parameters				
Total Quantum Efficiency (QE)	η	31	%	$\lambda = 545 \text{ nm}$
Inverse of Overall System Gain	$\frac{1}{K}$	5.5	$\frac{e^-}{DN}$	
Temporal Dark Noise	σ_{do}	30	e^-	
Saturation Capacity	$\mu_{e.sat}$	21100	e^-	
Derived Parameters				
Absolute Sensitivity Threshold	$\mu_{p.min}$	94	$p\sim$	$\lambda = 545 \text{ nm}$
Dynamic Range	$DYN_{out.bit}$	9.5	bit	
Maximum SNR	$SNR_{y.max.bit}$	7.2	bit	
	$SNR_{y.max.dB}$	43.2	dB	
Item	Symbol	Typ.	Unit	Remarks
Spatial Noise Parameters				
Spatial Offset Noise, $DSNU_{1288}$	σ_o	9.3	e^-	
Spatial Gain Noise, $PRNU_{1288}$	S_g	1.0	%	

Table 1: Most Important Specification Data

Operating Point		
Item	Symbol	Remarks
Video output format		12 bits/pixel(Mono16)
Gain	Register raw	0
Offset	Register raw	60
Exposure time	T_{exp}	80.0 μs to 17.5 ms

Table 2: Operating Point for the Camera Used

¹The unit e^- is used in this document as a statistically measured quantity.

2 Introduction

This measurement protocol describes the specification of Basler piA1900-32gm cameras. The measurement methods conform to the 1288 EMVA Standard, the Standard for Characterization and Presentation of Specification Data for Image Sensors and Cameras (Release A1.03) of the European Machine Vision Association (EMVA) [1].

The most important specification data for Basler piA1900-32gm cameras is summarized in table 1.

3 Basic Information

Basic Information	
Vendor	Basler
Model	piA1900-32gm
Type of data presented	Typical
Number of samples	1
Sensor	KAI-2093
Sensor type	CCD
Sensor diagonal	Diagonal 16.3 mm
Indication of lens category to be used	C-Mount
Resolution	1920 x 1084 pixel
Pixel width	7.40 μm
Pixel height	7.40 μm
Readout type	Progressive scan
Transfer type	Interline transfer
Shutter type	-
Overlap capabilities	Overlapping
Maximum readout rate	32 frames/second
General conventions	-
Interface type	Gigabit Ethernet

Table 3: Basic Information

3.1 Illumination

3.1.1 Illumination Setup for the Basler Camera Test Tool

The illumination during the testing on each camera was fixed. The drift in the illumination over a long period of time and after the lamp is changed is measured by a reference Basler A602fc camera. The reference camera provides an intensity factor that was used to calculate the irradiance for each camera measurement.

Light Source				
Item	Symbol	Typ.	Unit	Remarks
Wavelength	λ	545	nm	
Wavelength Variation	$\Delta\lambda$	50	nm	
Distance sensor to light source	d	280	mm	
Diameter of the light source	D	35	mm	
f-Number	$f_{\#}$	8		$f_{\#} = \frac{d}{D}$

Table 4: Light Source

3.1.2 Measurement of the Irradiance

The irradiance was measured using an IL1700 Radiometer from International Light Inc. (Detector: SEL033 #6285; Input optic: W #9461; Filter: F #21487; regular calibration). The accuracy of the Radiometer is specified as $\pm 3.5\%$.

The measured irradiance is plotted in figure 1.

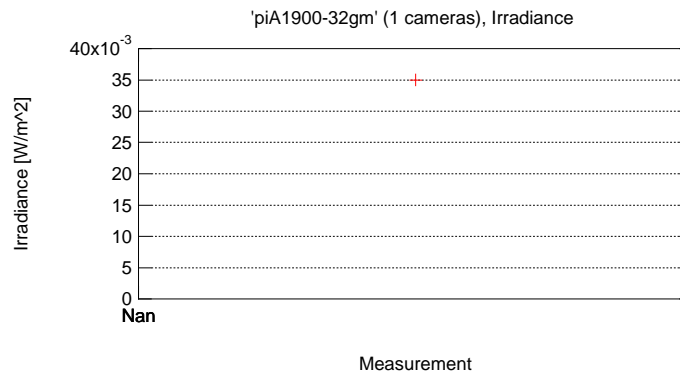


Figure 1: Irradiance for Each Camera Measurement.

The error for each calculated value using the amount of light falling on the sensor is dependent on the accuracy of the irradiance measurement.

4 Characterizing Temporal Noise and Sensitivity

4.1 Basic Parameters

4.1.1 Total Quantum Efficiency

Total Quantum Efficiency for One Fixed Wavelength Total quantum efficiency $\eta(\lambda)$ in [%] for monochrome light at $\lambda = 545 \text{ nm}$ with a wavelength variation of $\Delta\lambda = 50 \text{ nm}$.

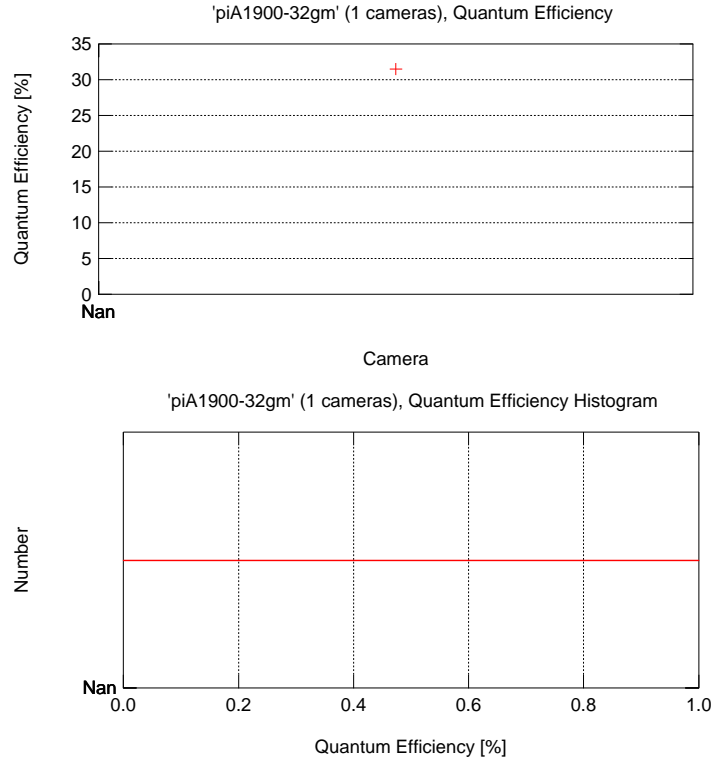


Figure 2: Total Quantum Efficiency (QE)

Item	Symbol	Typ.	Std. Dev.	Unit	Remarks
Total Quantum Efficiency (QE)	η	31	TBD	%	$\lambda = 545 \text{ nm}$

Table 5: Total Quantum Efficiency (QE)

The main error in the total quantum efficiency $\Delta\eta$ is related to the error in the measurement of the illumination as described in section 3.1.

Total Quantum Efficiency Versus Wavelength of the Light Total quantum efficiency $\eta(\lambda)$ in [%] for monochrome light versus wavelength of the light in [nm] .

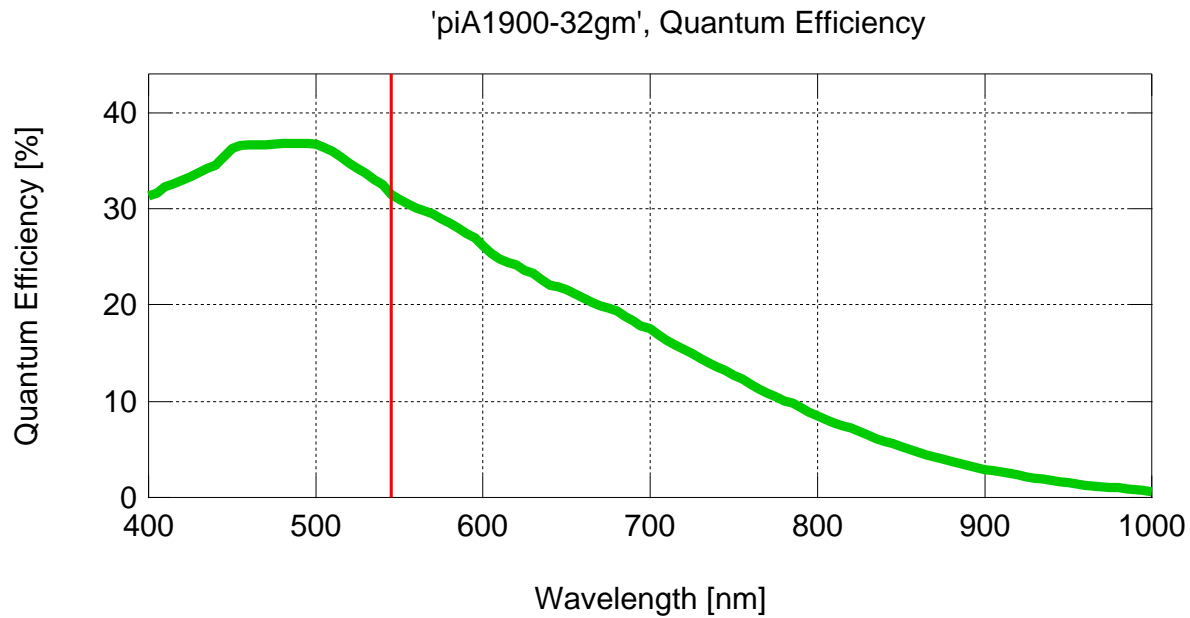


Figure 3: Total Quantum Efficiency Versus Wavelength of the Light

The curve of the total quantum efficiency versus the wavelength as shown in figure 3 was calculated from the single measured total quantum efficiency as presented in section 4.1.1. For the shape of the curve, the data from the sensor data sheet was used.

4.1.2 Temporal Dark Noise

Standard deviation of the temporal dark noise σ_{d_0} referenced to electrons for exposure time zero in $[e^-]$.

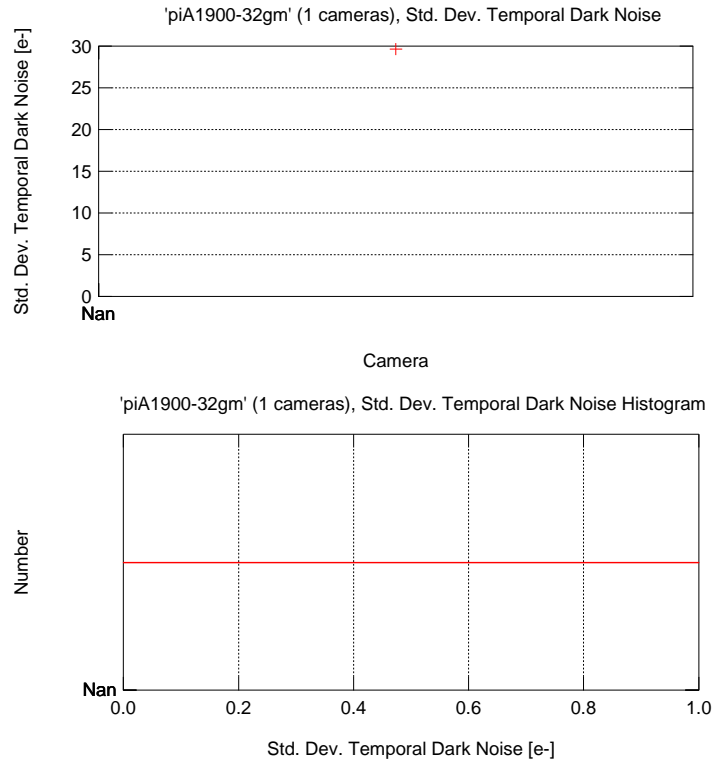


Figure 4: Temporal Dark Noise

Item	Symbol	Typ.	Std. Dev.	Unit	Remarks
Temporal Dark Noise	σ_{d_0}	30	Nan	e^-	

Table 6: Temporal Dark Noise

4.1.3 Dark Current

Dark current N_{d30} for a housing temperature of 30° C in $[e^-/s]$.
Not measured!

4.1.4 Doubling Temperature

Doubling temperature k_d of the dark current in $[^\circ\text{C}]$.
Not measured!

4.1.5 Inverse of Overall System Gain

Inverse of overall system gain $\frac{1}{K}$ in $[\frac{e^-}{DN}]$.

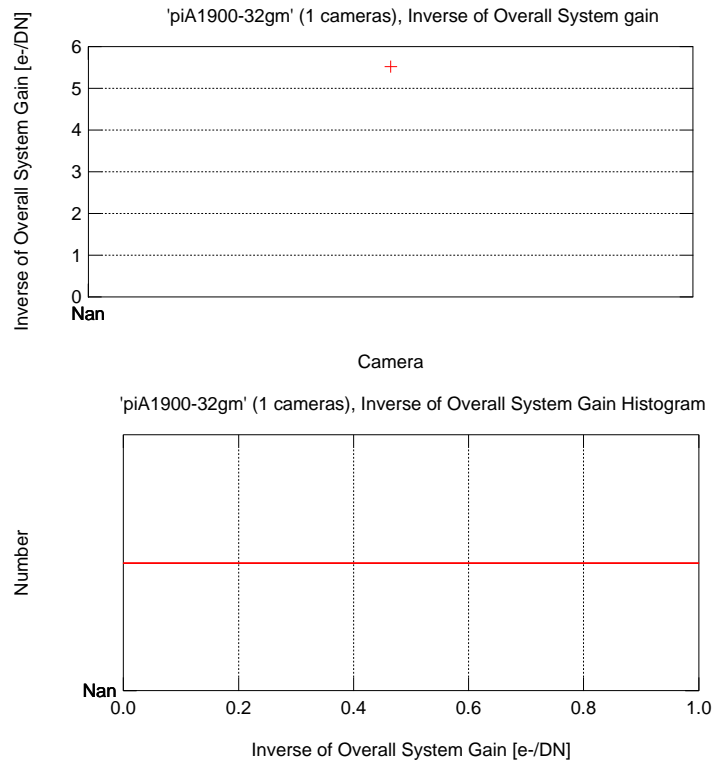


Figure 5: Inverse of Overall System Gain

Item	Symbol	Typ.	Std. Dev.	Unit	Remarks
Inverse of Overall System Gain	$\frac{1}{K}$	5.5	Nan	$\frac{e^-}{DN}$	

Table 7: Inverse of Overall System Gain

4.1.6 Inverse Photon Transfer

Inverse photon transfer $\frac{1}{\eta K}$ in $\left[\frac{p \sim}{DN} \right]$.

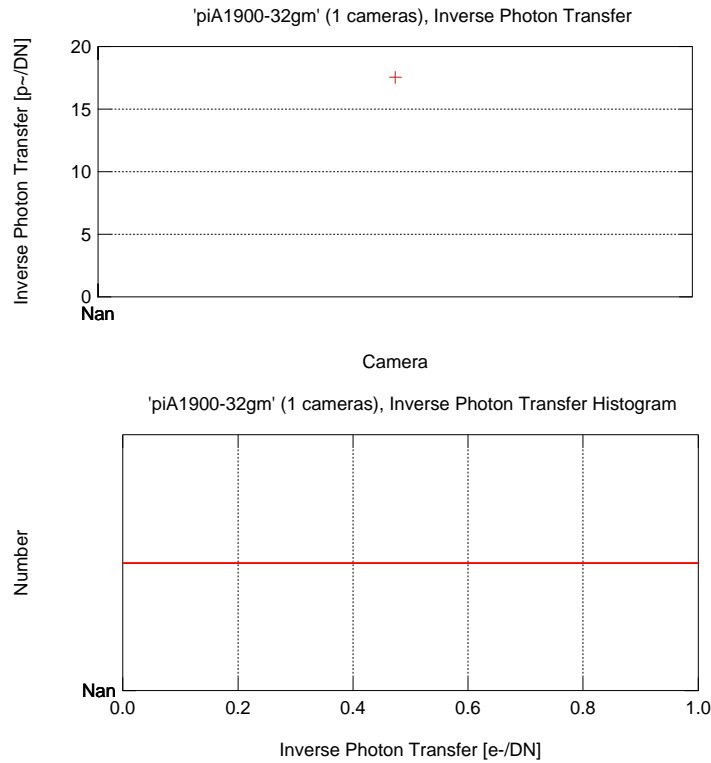


Figure 6: Inverse Photon Transfer

Item	Symbol	Typ.	Std. Dev.	Unit	Remarks
Inverse Photon Transfer	$\frac{1}{\eta K}$	17.5	TBD	$\frac{p \sim}{DN}$	$\lambda = 545 \text{ nm}$

Table 8: Inverse Photon Transfer

The main error in the inverse photon transfer $\frac{1}{\eta K}$ is related to the error in the measurement of the illumination as described in section 3.1.

4.1.7 Saturation Capacity

Saturation capacity $\mu_{e.sat}$ referenced to electrons in $[e^-]$.

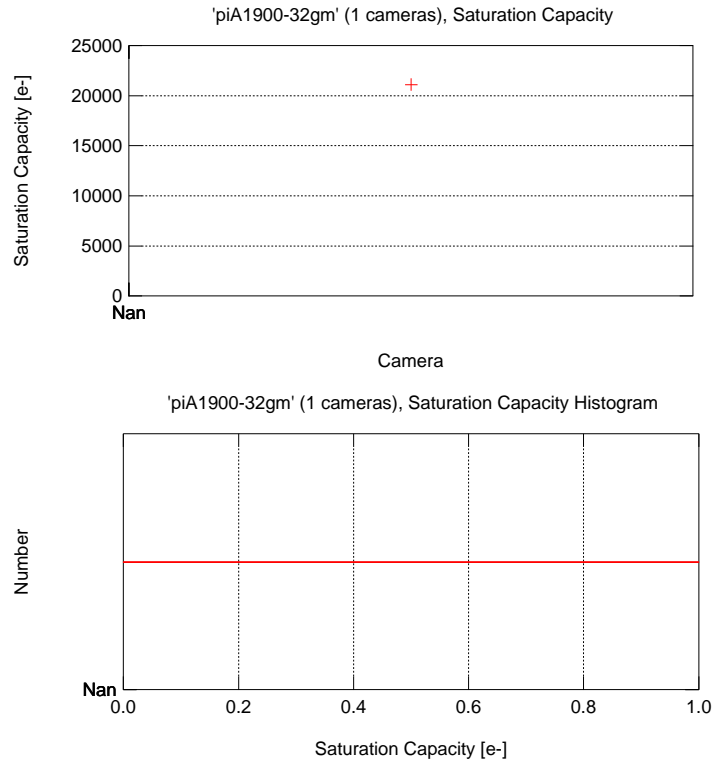


Figure 7: Saturation Capacity

Item	Symbol	Typ.	Std. Dev.	Unit	Remarks
Saturation Capacity	$\mu_{e.sat}$	21100	Nan	e^-	

Table 9: Saturation Capacity

4.1.8 Spectrogram

Spectrogram referenced to photons in $[p\sim]$ is plotted versus spatial frequency in $[1/\text{pixel}]$ for no light, 50% saturation, and 90% saturation.

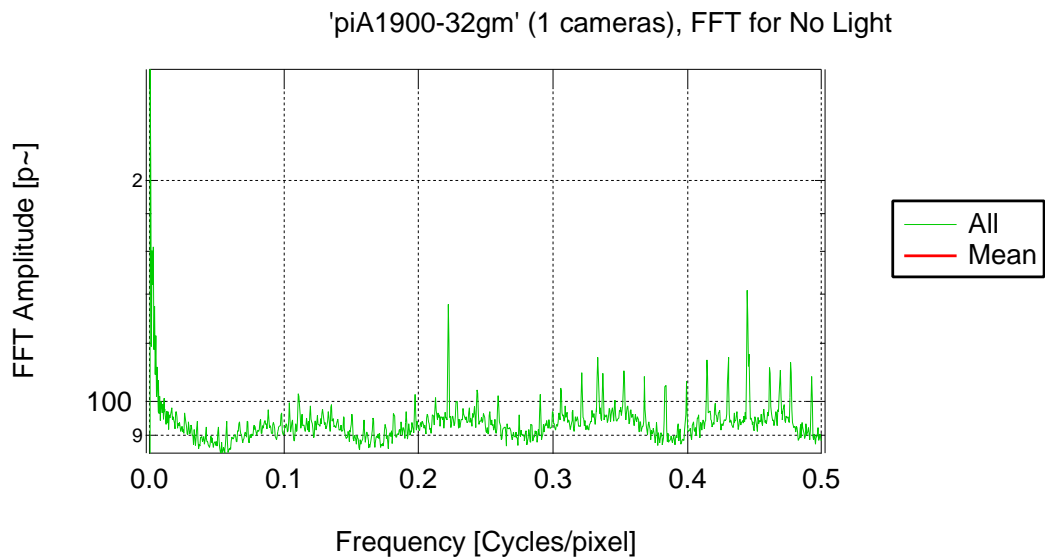
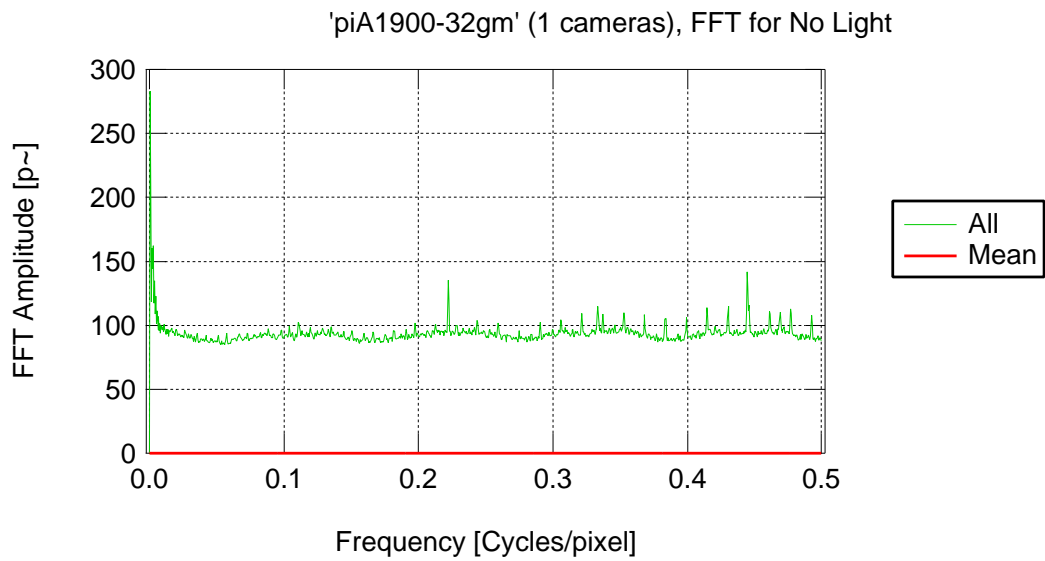


Figure 8: Spectrogram Referenced to Photons for No Light

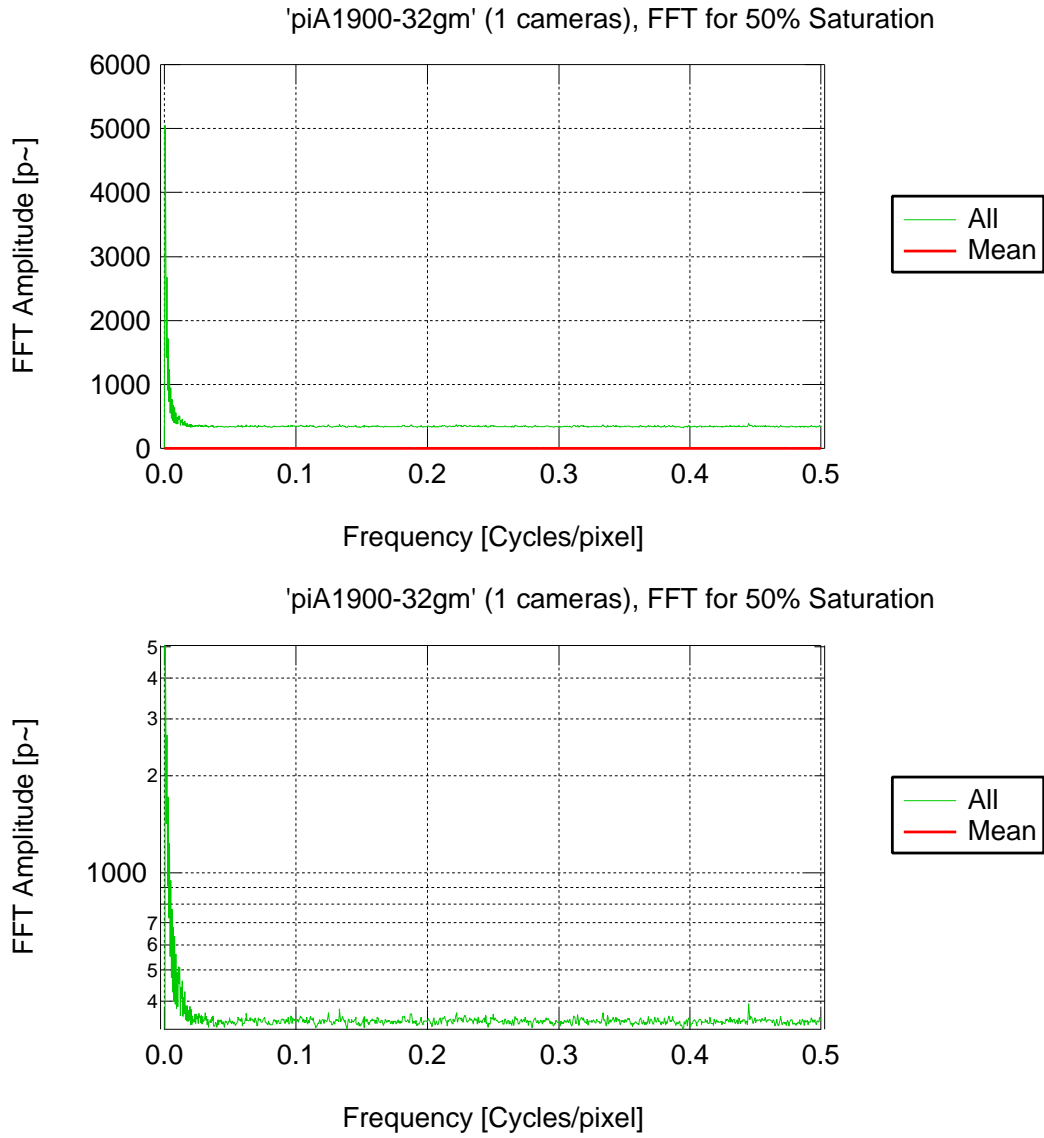


Figure 9: Spectrogram Referenced to Photons for 50% Saturation

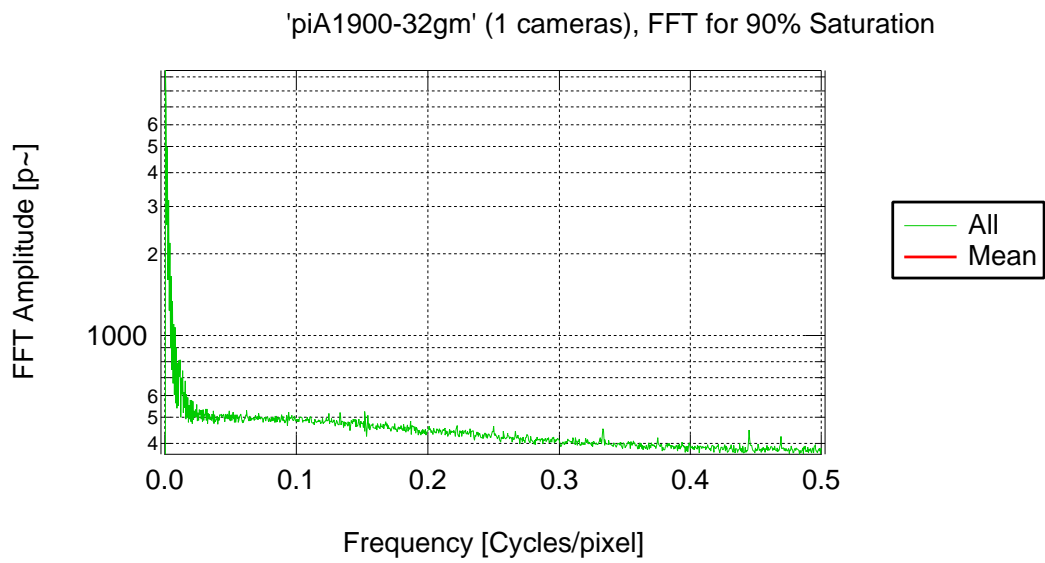
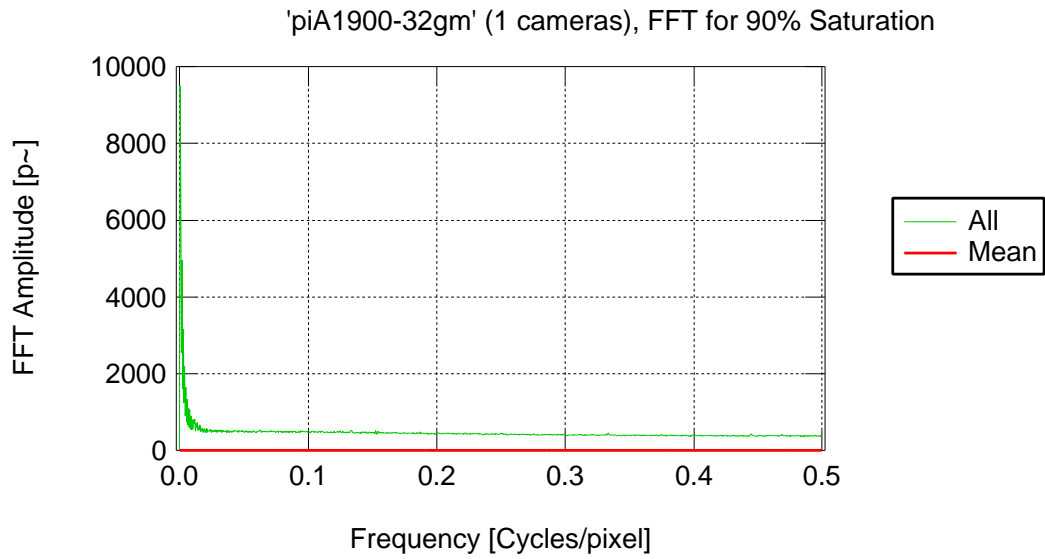


Figure 10: Spectrogram Referenced to Photons for 90% Saturation

4.1.9 Non-Whiteness Coefficient

The non-whiteness coefficient is plotted versus the number of photons μ_p in $[p^\sim]$ collected in a pixel during exposure time.

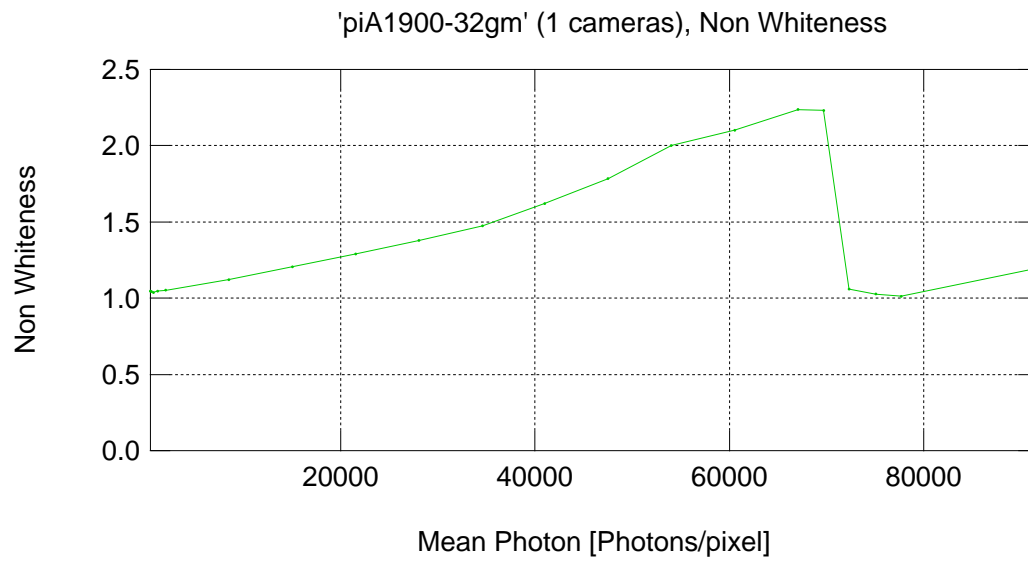


Figure 11: Non-whiteness Coefficient

4.2 Derived Data

4.2.1 Absolute Sensitivity Threshold

Absolute sensitivity threshold $\mu_{p.min}(\lambda)$ in $[p\sim]$ for monochrome light versus wavelength of the light in $[nm]$.

$$\mu_{p.min} = \frac{\sigma_{d_0}}{\eta} \tag{1}$$

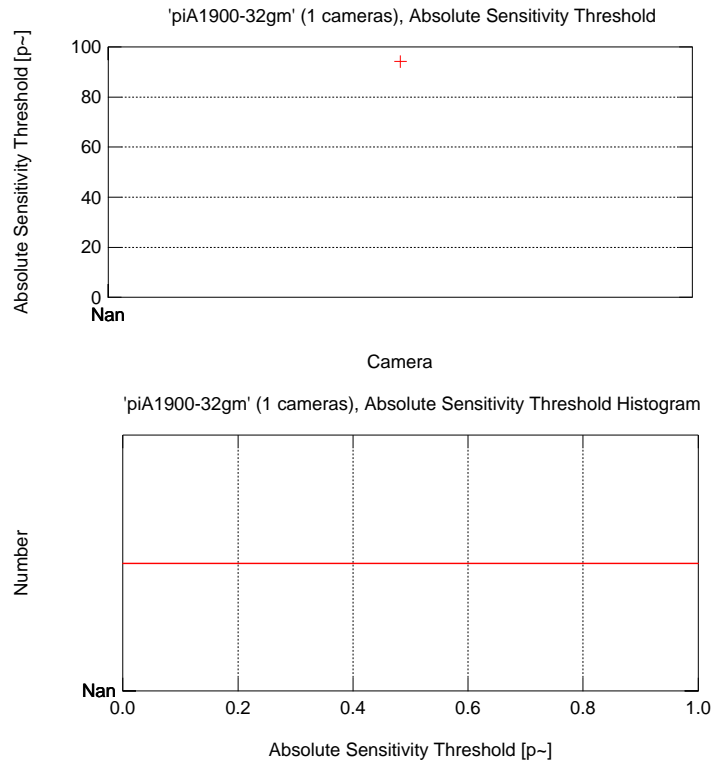


Figure 12: Absolute Sensitivity Threshold

Item	Symbol	Typ.	Std. Dev.	Unit	Remarks
Absolute Sensitivity Threshold	$\mu_{p.min}$	94	TBD	$p\sim$	$\lambda = 545 \text{ nm}$

Table 10: Absolute Sensitivity Threshold

4.2.2 Signal-to-noise Ratio

Signal-to-noise ratio $\text{SNR}_y(\mu_p)$ is plotted versus number of photons μ_p collected in a pixel during exposure time in $[\text{p}^\sim]$ for monochrome light with the wavelength λ given in $[\text{nm}]$. The wavelength should be near the maximum of the quantum efficiency.

$$A : \text{SNR}_y = \frac{\mu_y - \mu_{y,\text{dark}}}{\sigma_y} \quad (2)$$

$$B : \text{SNR}_y = \frac{\eta\mu_p}{\sqrt{(\eta\mu_p + \sigma_{d_0}^2)}} \quad (3)$$

Figure 13 shows the signal-to-noise ratio SNR_y for monochrome light with the wavelength $\lambda = 545 \text{ nm}$.

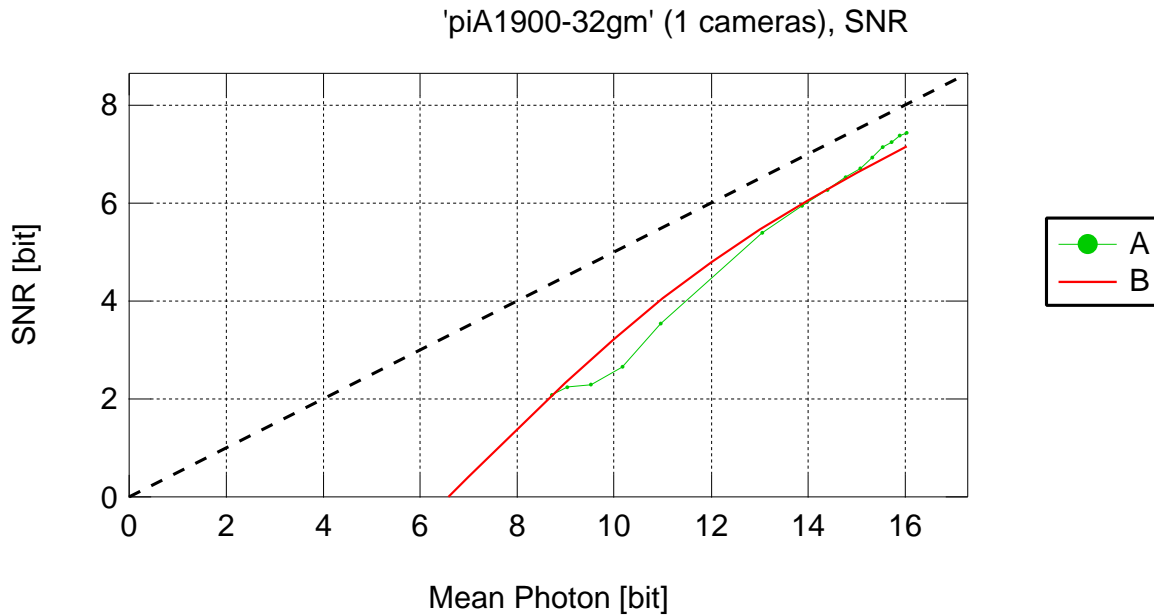


Figure 13: Signal-to-noise Ratio

The maximum achievable image quality is given as $\text{SNR}_{y,\text{max}}$.

$$\text{SNR}_{y,\text{max}} = \sqrt{\mu_{e,\text{sat}}} \quad (4)$$

$$\text{SNR}_{y,\text{max},\text{bit}} = \text{ld } \text{SNR}_{y,\text{max}} = \frac{\log \text{SNR}_{y,\text{max}}}{\log 2} \quad (5)$$

$$\text{SNR}_{y,\text{max},\text{dB}} = 20 \log \text{SNR}_{y,\text{max}} \approx 6.02 \text{SNR}_{y,\text{max},\text{bit}} \quad (6)$$

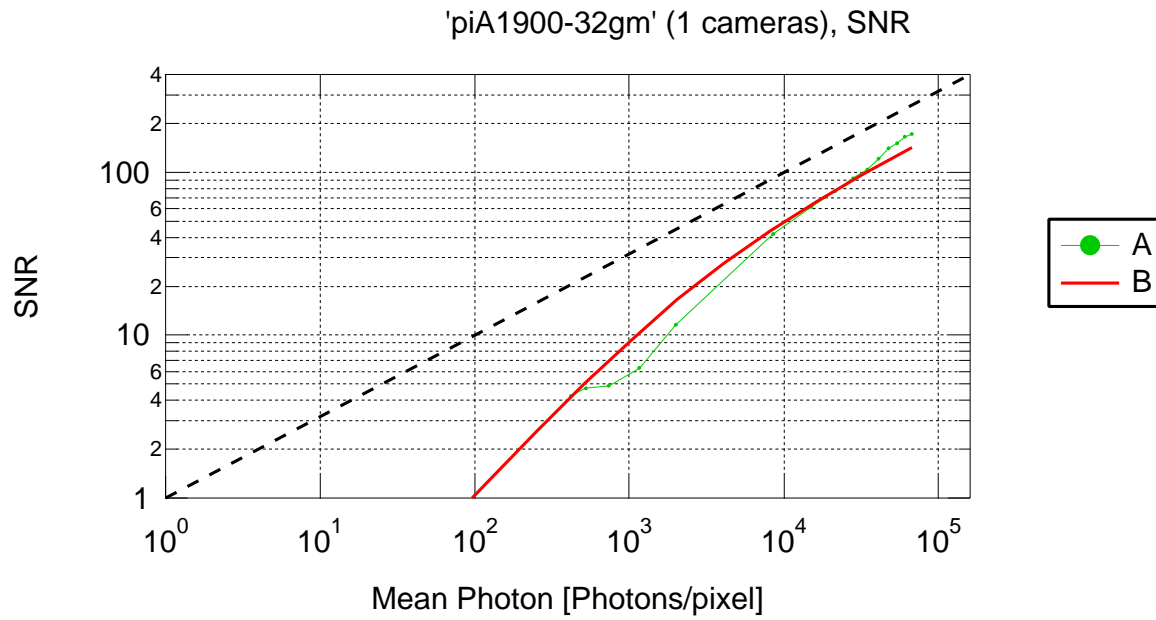


Figure 14: Signal-to-noise Ratio

Item	Symbol	Typ.	Std. Dev.	Unit	Remarks
Maximum achievable SNR [bit]	$SNR_{y,max.bit}$	7.2	Nan	bit	

Table 11: Maximum achievable SNR [bit]

Item	Symbol	Typ.	Std. Dev.	Unit	Remarks
Maximum achievable SNR [dB]	$SNR_{y,max.dB}$	43.2	Nan	dB	

Table 12: Maximum achievable SNR [dB]

4.2.3 Dynamic Range

Dynamic range $DYN_{out.bit}$ in [bit].

$$DYN_{out} = \frac{\mu_{e.sat}}{\sigma_{d_0}} \tag{7}$$

$$DYN_{out.bit} = \log_2(DYN_{out}) \tag{8}$$

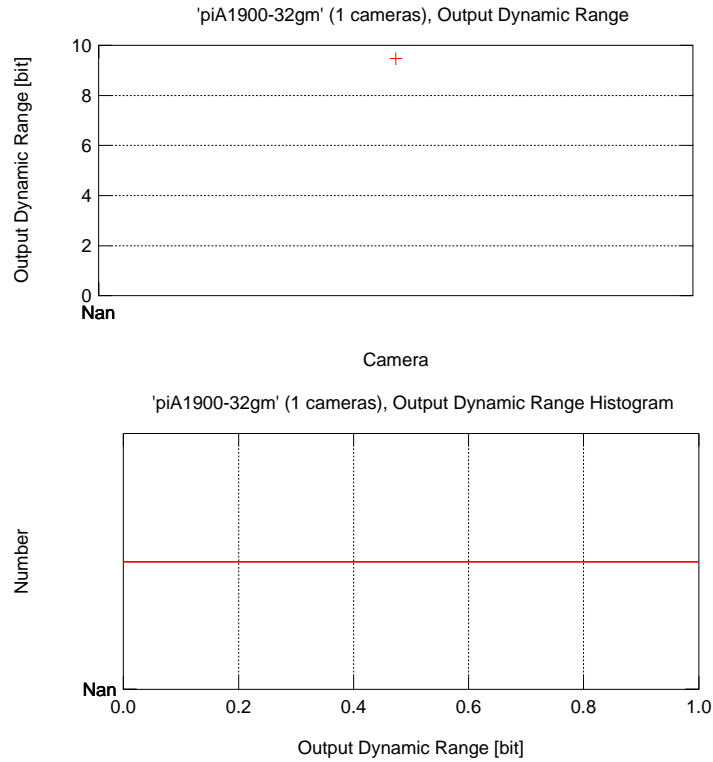


Figure 15: Output Dynamic Range

Item	Symbol	Typ.	Std. Dev.	Unit	Remarks
Output Dynamic Range	$DYN_{out.bit}$	9.5	Nan	bit	

Table 13: Output Dynamic Range

4.3 Raw Measurement Data

4.3.1 Mean Gray Value

Mean gray value $\mu_y(\mu_p)$ in [DN] is plotted versus number of photons μ_p in [p \sim] collected in a pixel during exposure time.

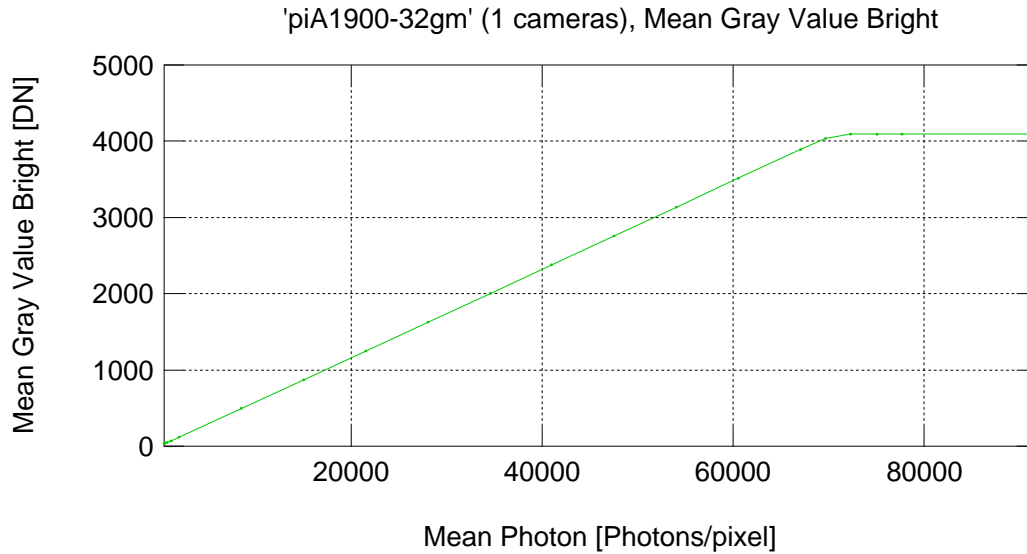


Figure 16: Mean Gray Values of the Cameras with Illuminated Pixels

4.3.2 Variance of the Temporal Distribution of Gray Values

The variance of the temporal distribution of gray values $\sigma_{y,temp}^2(\mu_p)$ in $[\text{DN}^2]$ is plotted versus number of photons μ_p in $[\tilde{p}]$ collected in a pixel during exposure time.

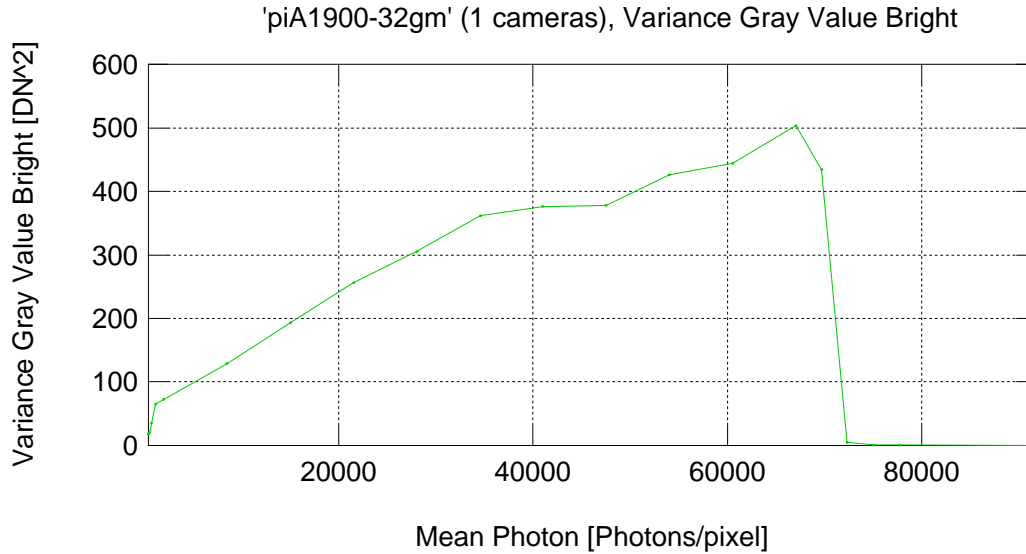


Figure 17: Variance Values for the Temporal Distribution of Gray Values with Illuminated Pixels

Saturation Capacity The saturation point is defined as the maximum of the curve in figure 17. The abscissa of the maximum point is the number of photons $\mu_{p.sat}$ where the camera saturates. The saturation capacity $\mu_{e.sat}$ in electrons is computed according to the mathematical model as:

$$\mu_{e.sat} = \eta \mu_{p.sat} \quad (9)$$

4.3.3 Mean of the Gray Values Dark Signal

Mean of the gray values dark signal $\mu_{y.dark}(T_{exp})$ in [DN] is plotted versus exposure time in [s].

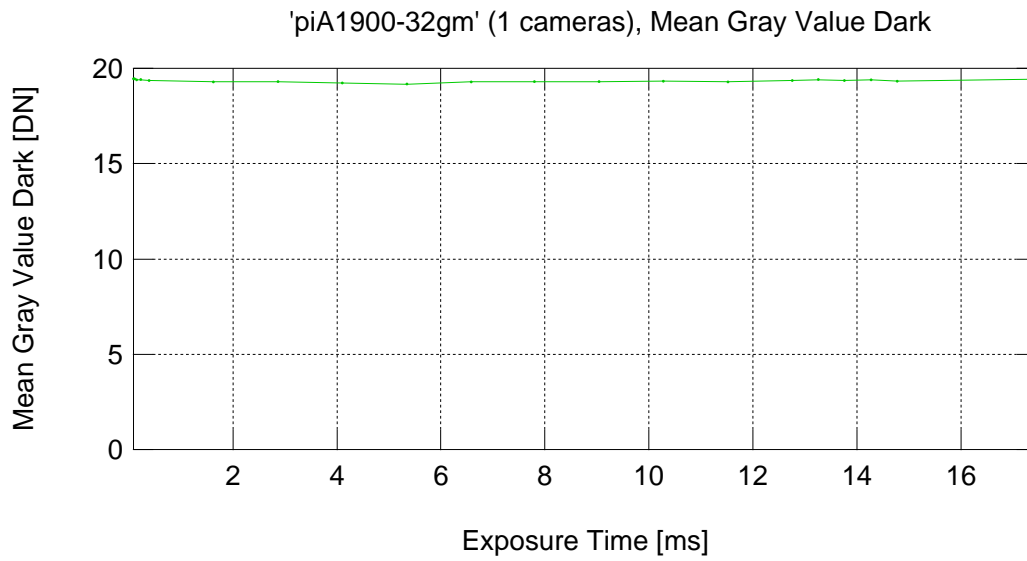


Figure 18: Mean Gray Values for the Cameras in Darkness

4.3.4 Variance of the Gray Value Temporal Distribution in Darkness

The variance of the temporal distribution of gray values in darkness $\sigma_{y.temp.dark}^2(T_{exp})$ in $[DN^2]$ is plotted versus exposure time T_{exp} in $[s]$.

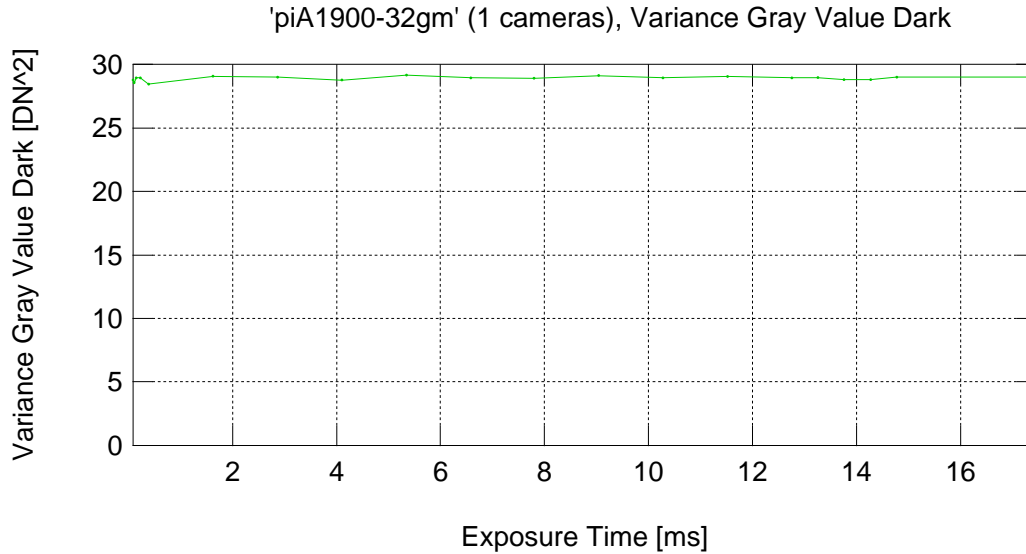


Figure 19: Variance Values for the Temporal Distribution of Gray Values in Darkness

Temporal Dark Noise The dark noise for exposure time zero is found as the offset of the linear correspondence in figure 19. Match a line (with offset) to the linear part of the data in the diagram. The dark noise for exposure time zero $\sigma_{d_0}^2$ is found as the offset of the line divided by the square of the overall system gain K .

$$\sigma_{d_0} = \sqrt{\frac{\sigma_{y.temp.dark}^2(T_{exp} = 0)}{K^2}} \quad (10)$$

4.3.5 Light Induced Variance of the Temporal Distribution of Gray Values

The light induced variance of the temporal distribution of gray values in $[DN^2]$ is plotted versus light induced mean gray value in $[DN]$.

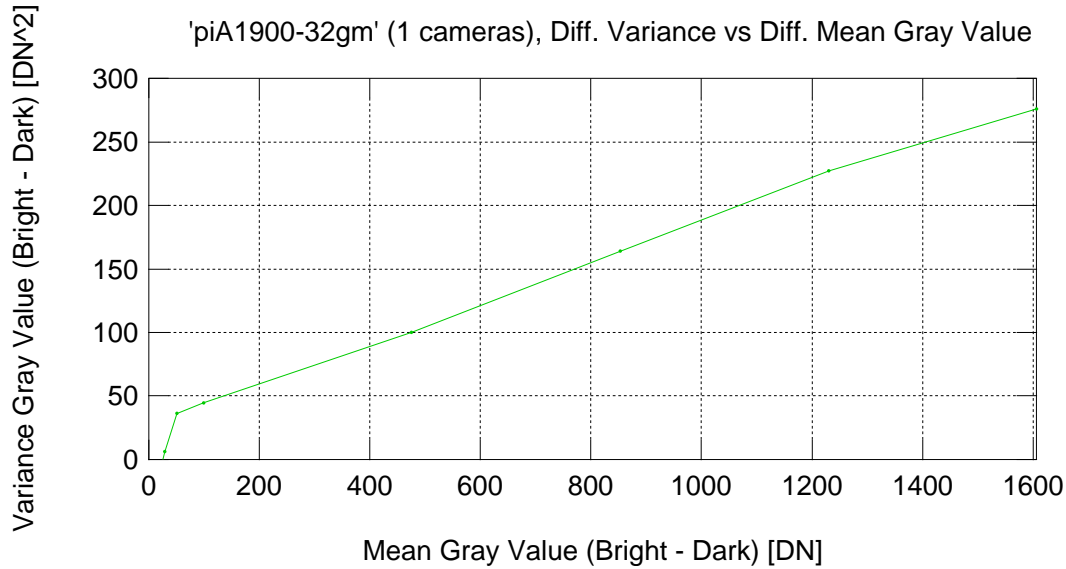


Figure 20: Light Induced Variance of the Temporal Distribution of Gray Values Versus Light Induced Mean Gray Value

Overall System Gain The overall system gain K is computed according to the mathematical model as:

$$K = \frac{\sigma_{y.temp}^2 - \sigma_{y.temp.dark}^2}{\mu_y - \mu_{y.dark}} \quad (11)$$

which describes the linear correspondence in figure 20. Match a line starting at the origin to the linear part of the data in this diagram. The slope of this line is the overall system gain K .

4.3.6 Light Induced Mean Gray Value

The light induced mean gray value $\mu_y - \mu_{y.dark}$ in [DN] is plotted versus the number of photons collected in a pixel during exposure time $K\mu_p$ in [p \sim].

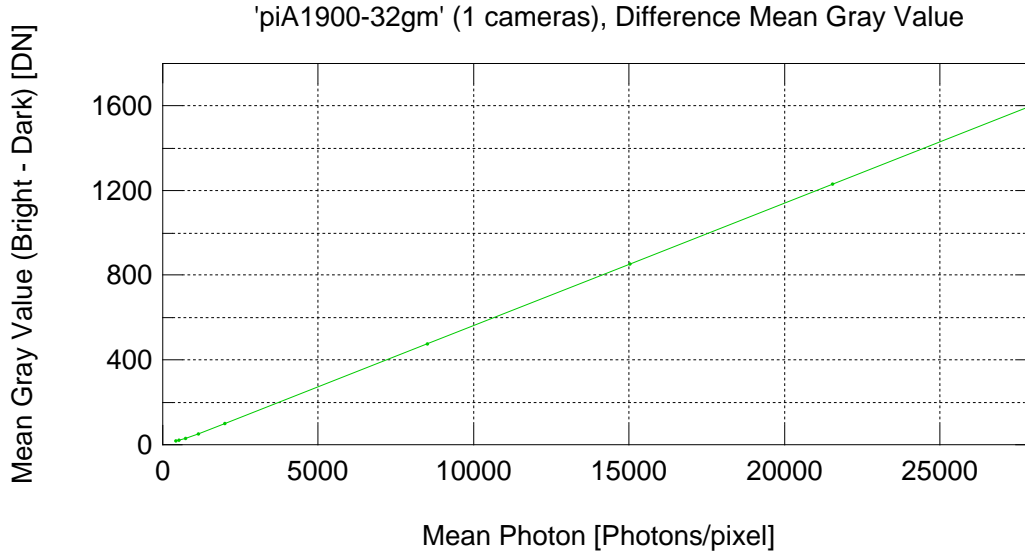


Figure 21: Light Induced Mean Gray Value Versus the Number of Photons

Total Quantum Efficiency The total quantum efficiency η is computed according to the mathematical model as:

$$\eta = \frac{\mu_y - \mu_{y.dark}}{K\mu_p} \quad (12)$$

which describes the linear correspondence in figure 21. Match a line starting at the origin to the linear part of the data in this diagram. The slope of this line divided by the overall system gain K yields the total quantum efficiency η .

The number of photons μ_p is calculated using the model for monochrome light. The number of photons Φ_p collected in the geometric pixel per unit exposure time [p \sim /s] is given by:

$$\Phi_p = \frac{EA\lambda}{hc} \quad (13)$$

with the irradiance E on the sensor surface [W/m²], the area A of the (geometrical) pixel [m²], the wavelength λ of light [m], the Planck's constant $h \approx 6.63 \cdot 10^{-34}$ Js, and the speed of light $c \approx 3 \cdot 10^8$ m/s. The number of photons can be calculated by:

$$\mu_p = \Phi_p T_{exp} \quad (14)$$

during the exposure time T_{exp} . Using equation 12 and the number of photons μ_p , the total quantum efficiency η can be calculated as:

$$\eta = \frac{hc}{AT_{exp}} \frac{1}{E} \frac{1}{\lambda} \frac{\mu_p - \mu_{y.dark}}{K} \quad (15)$$

4.3.7 Dark Current Versus Housing Temperature

The logarithm to the base 2 of the dark current in $[e^-/s]$ versus deviation of the housing temperature from 30°C in $[^\circ\text{C}]$

Not measured!

5 Characterizing Total and Spatial Noise

5.1 Basic Parameters

5.1.1 Spatial Offset Noise

Standard deviation of the spatial offset noise σ_o referenced to electrons in $[e^-]$.

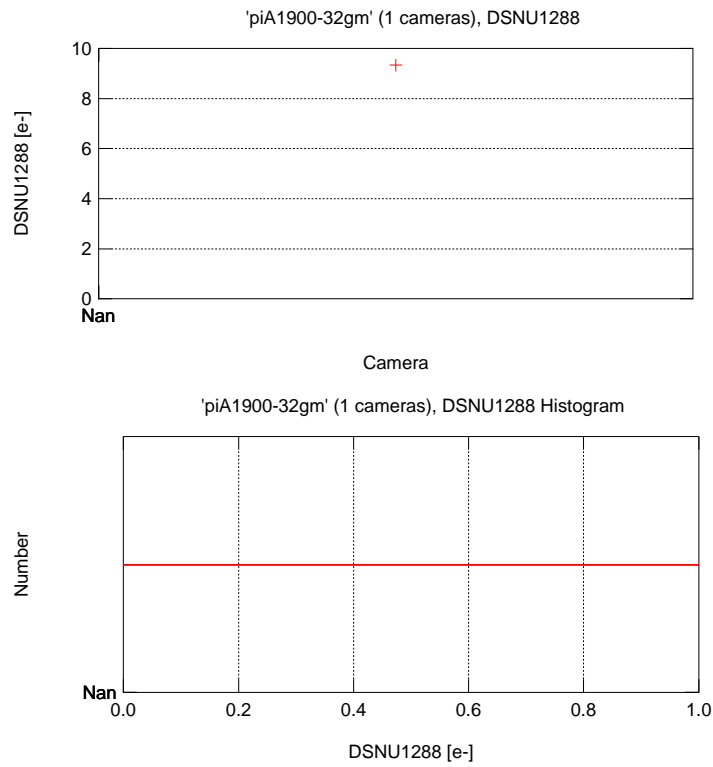


Figure 22: Spatial Offset Noise ($DSNU_{1288}$)

Item	Symbol	Typ.	Std. Dev.	Unit	Remarks
Spatial Offset Noise ($DSNU_{1288}$)	σ_o	9.3	Nan	e^-	

Table 14: Spatial Offset Noise ($DSNU_{1288}$)

5.1.2 Spatial Gain Noise

Standard deviation of the spatial gain noise S_g in [%].

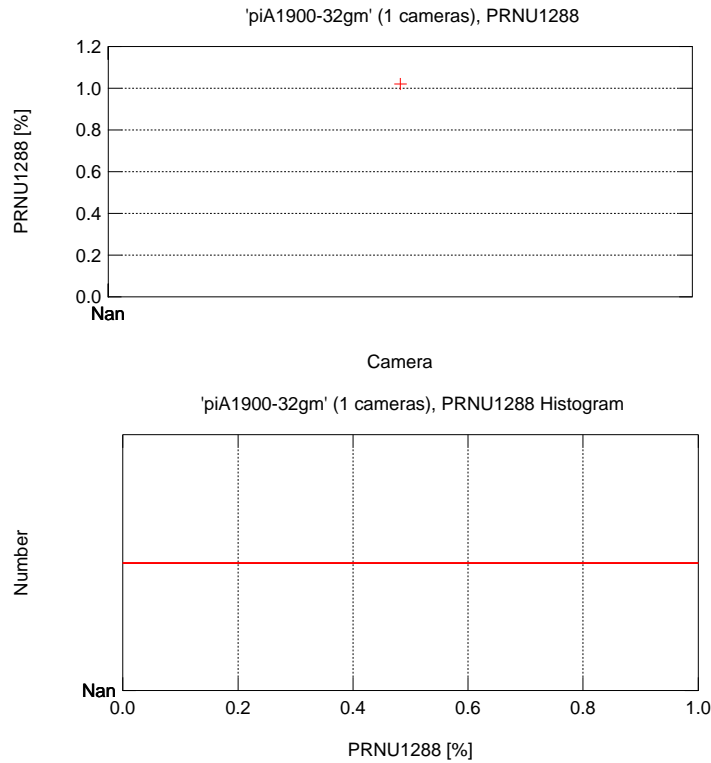


Figure 23: Spatial Gain Noise ($PRNU_{1288}$)

Item	Symbol	Typ.	Std. Dev.	Unit	Remarks
Spatial Gain Noise ($PRNU_{1288}$)	S_g	1.0	Nan	%	

Table 15: Spatial Gain Noise ($PRNU_{1288}$)

5.1.3 Spectrogram Spatial Noise

Spectrogram referenced to photons in $[p\sim]$ is plotted versus spatial frequency in $[1/\text{pixel}]$ for no light, 50% saturation, and 90% saturation.

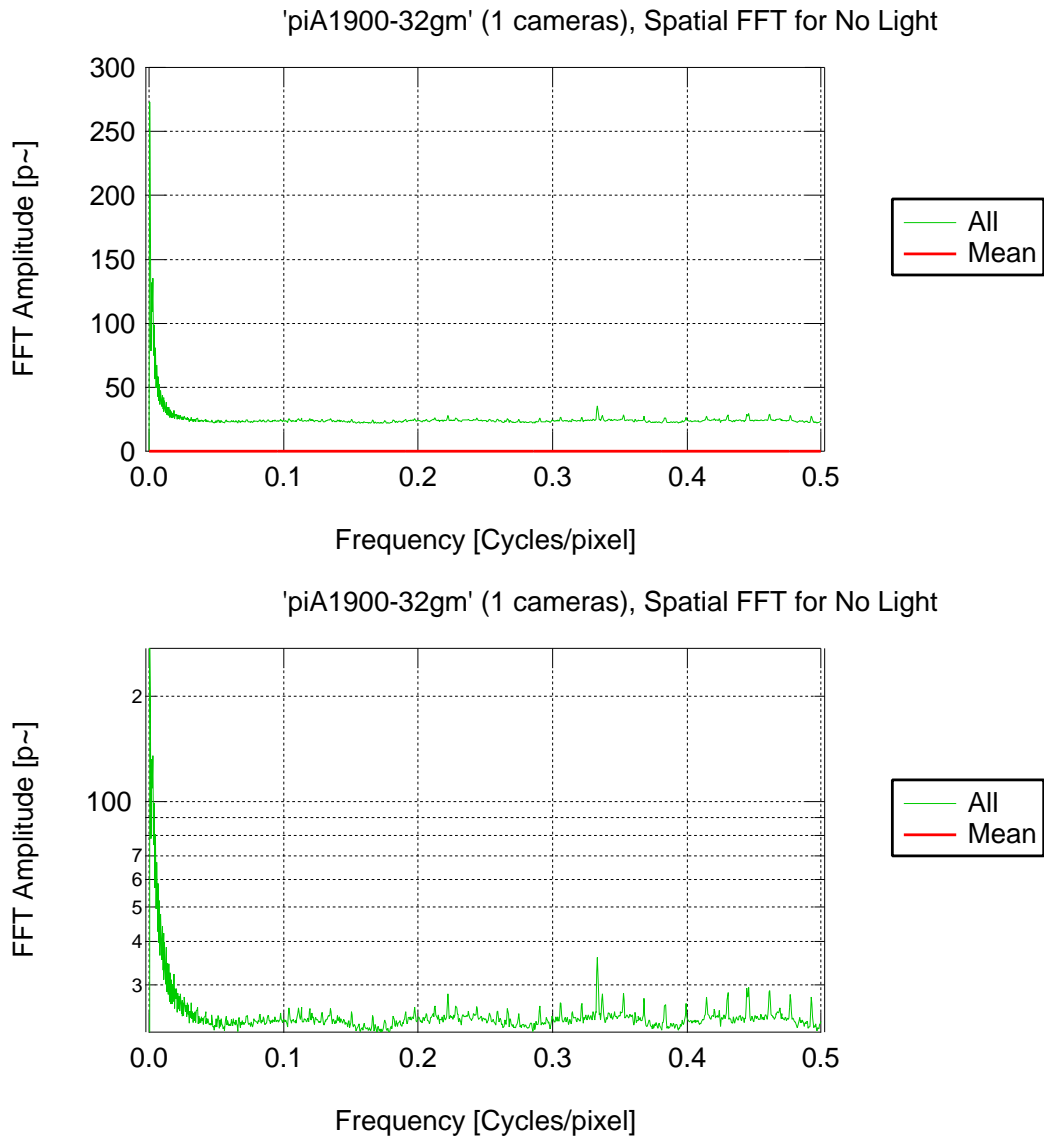


Figure 24: Spectrogram Referenced to Photons for No Light

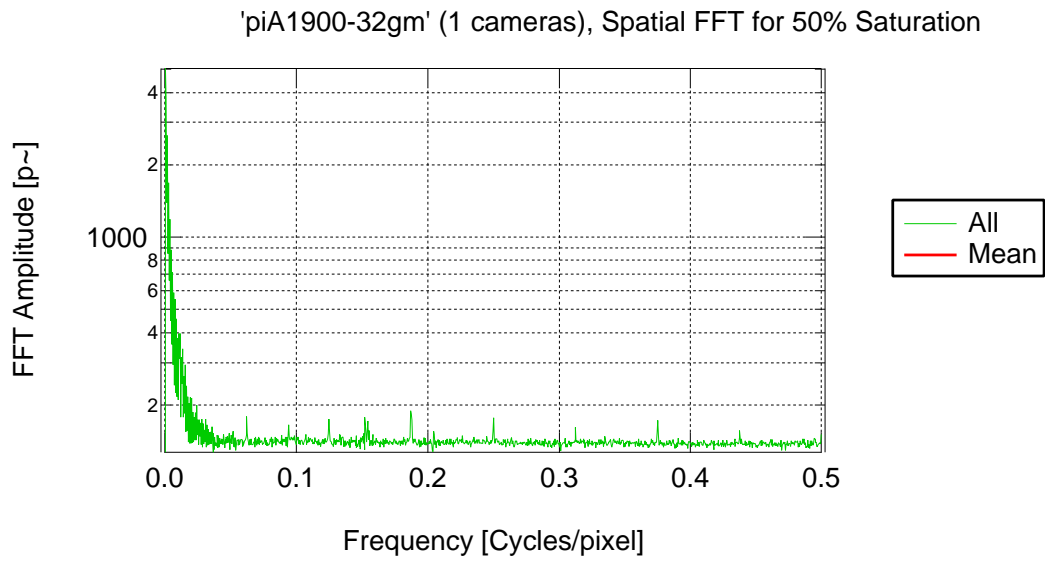
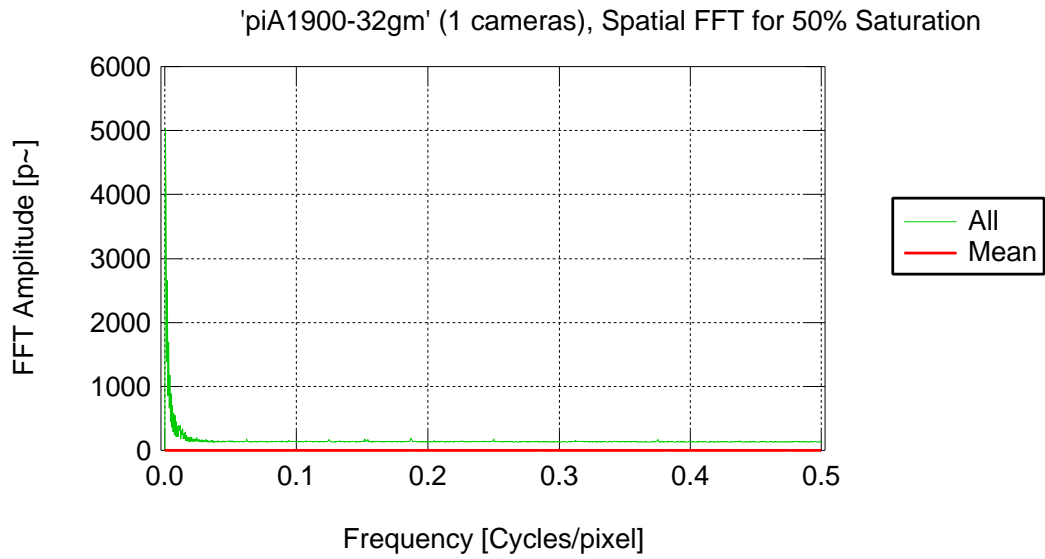


Figure 25: Spectrogram Referenced to Photons for 50% Saturation

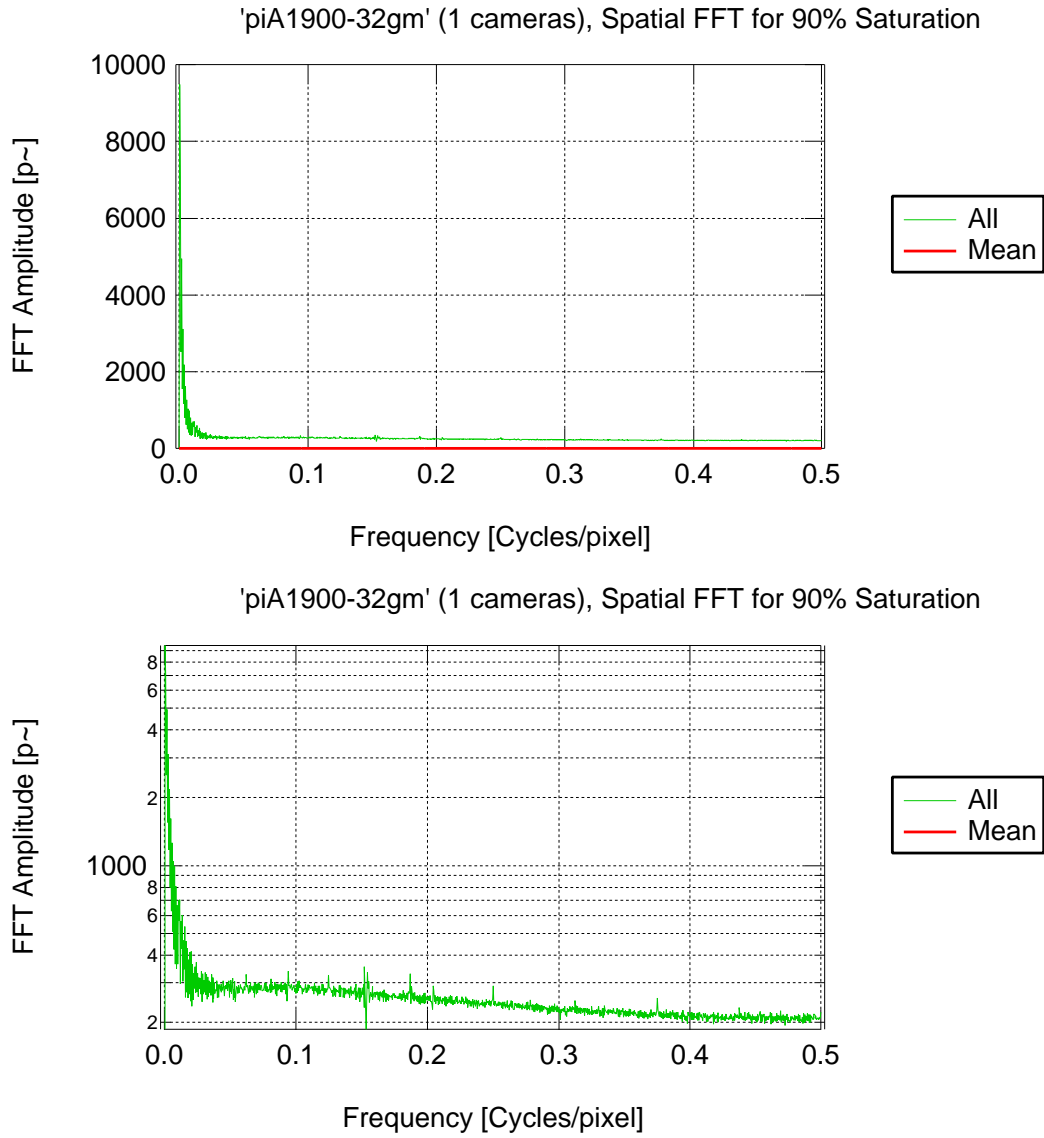


Figure 26: Spectrogram Referenced to Photons for 90% Saturation

5.1.4 Spatial Non-whiteness Coefficient

The non-whiteness coefficient is plotted versus the number of photons μ_p in $[p^\sim]$ collected in a pixel during exposure time.

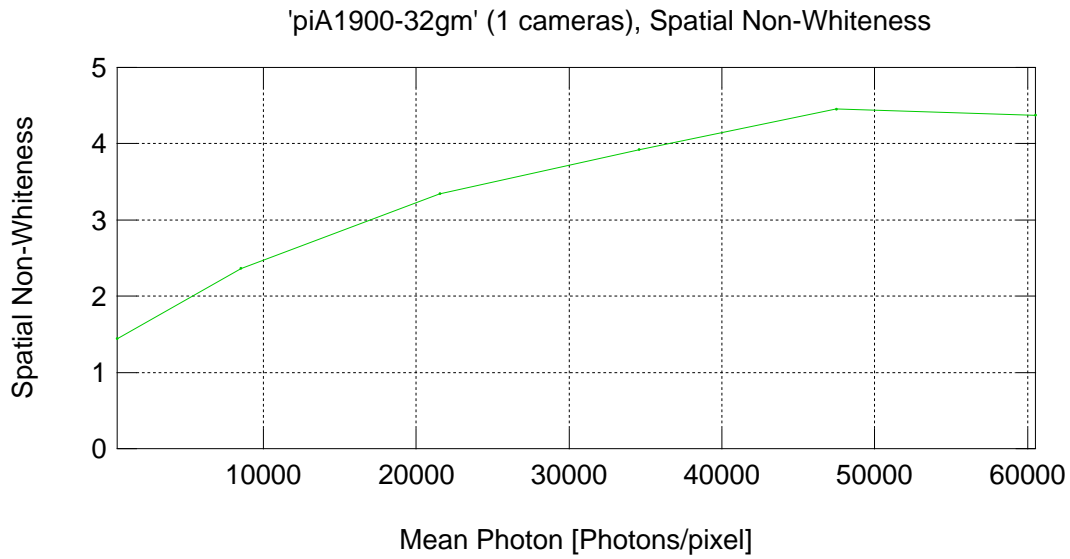


Figure 27: Spatial Non-whiteness Coefficient

5.2 Raw Measurement Data

5.2.1 Standard Deviation of the Spatial Dark Noise

Standard deviation of the spatial dark noise in [DN] versus exposure time in [s] .

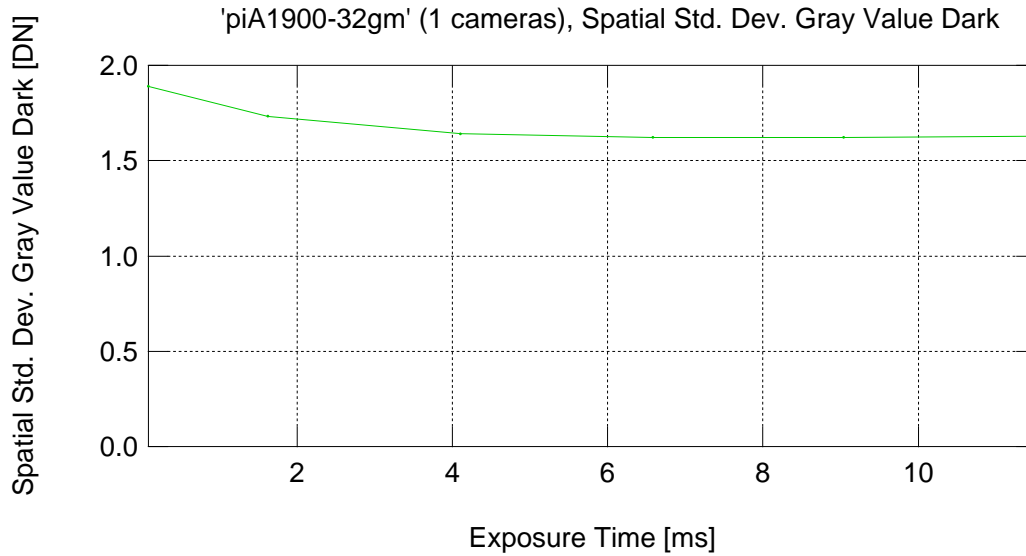


Figure 28: Standard Deviation of the Spatial Dark Noise

From the mathematical model, it follows that the **variance of the spatial offset noise** σ_o^2 should be constant and not dependent on the exposure time. Check that the data in the figure 28 forms a flat line. Compute the mean of the values in the diagram. The mean divided by the conversion gain K gives the standard deviation of the spatial offset noise σ_o .

$$\text{DSNU}_{1288} = \sigma_o = \frac{\sigma_{y.spat.dark}}{K} \quad (16)$$

The square of the result equals the variance of the spatial offset noise σ_o^2 .

5.2.2 Light Induced Standard Deviation of the Spatial Noise

Light induced standard deviation of the spatial noise in [DN] versus light induced mean of gray values [DN] .

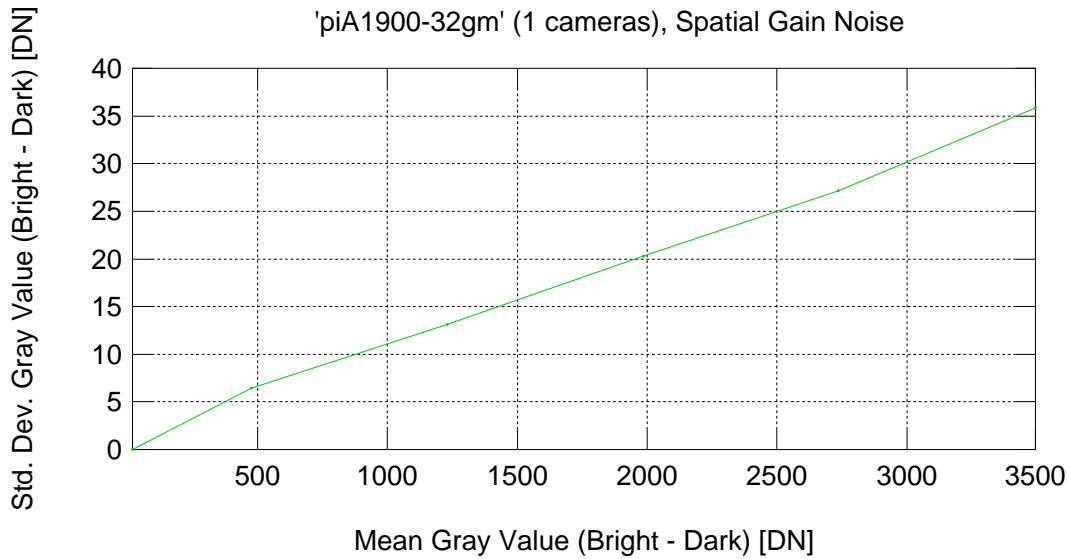


Figure 29: Light Induced Standard Deviation of the Spatial Noise

The **variance coefficient of the spatial gain noise** S_g^2 or its standard deviation value S_g respectively, is computed according to the mathematical model as:

$$\text{PRNU}_{1288} = S_g = \frac{\sqrt{\sigma_{y.spac}^2 - \sigma_{y.spac.dark}^2}}{\mu_y - \mu_{y.dark}}, \quad (17)$$

which describes the linear correspondence in figure 29. Match a line through the origin to the linear part of the data. The line's slope equals the standard deviation value of the spatial gain noise S_g .

References

- [1] EUROPEAN MACHINE VISION ASSOCIATION (EMVA): *EMVA Standard 1288 - Standard for Characterization and Presentation of Specification Data for Image Sensors and Cameras (Release A1.03)*. 2006